Mapping the Membrane Topology and Extracellular Ligand Binding Domains of the Retinol Binding Protein Receptor[†]

Riki Kawaguchi,[‡,§] Jiamei Yu,[‡,§] Patrick Wiita,[‡] Mariam Ter-Stepanian,[‡] and Hui Sun*[,‡,§,||]

Department of Physiology, Jules Stein Eye Institute, and Brain Research Institute, David Geffen School of Medicine at UCLA, Los Angeles, California 90095

Received February 4, 2008; Revised Manuscript Received March 25, 2008

ABSTRACT: STRA6 is a multitransmembrane domain protein not homologous to any other proteins with known function. It functions as the high-affinity receptor for plasma retinol binding protein (RBP) and mediates cellular uptake of vitamin A from the vitamin A−RBP complex. Consistent with the diverse roles of vitamin A and the wide tissue expression pattern of STRA6, mutations in STRA6 are associated with severe pathological phenotypes in humans. The structural basis for STRA6's biochemical function is unknown. Although computer programs predict 11 transmembrane domains for STRA6, its topology has never been studied experimentally. Elucidating the transmembrane topology of STRA6 is critical for understanding its structure and function. By inserting an epitope tag into all possible extracellular and intracellular domains of STRA6, we systematically analyzed the accessibility of each tag on the surface of live cells, the accessibility of each tag in permeabilized cells, and the effect of each tag on RBP binding and STRA6-mediated vitamin A uptake from the vitamin A−RBP complex. In addition, we used a new lysine accessibility technique combining cell-surface biotinylation and tandem-affinity purification to study a region of the protein not revealed by the epitope tagging method. These studies not only revealed STRA6's extracellular, transmembrane, and intracellular domains but also implicated extracellular regions of STRA6 in RBP binding.

Vitamin A and its derivatives (retinoids) are essential for diverse aspects of vertebrate physiology (*1*−*3*). Due to the hydrophobic nature of retinoids, it has been assumed that random diffusion is the primary, if not the only, means of transmembrane transport. However, biochemical evidence suggests that uptake of retinol from the small intestine is mediated by a membrane transporter (*4*). There is also strong evidence of the existence of a specific mechanism for transporting 11-*cis*-retinal in the retinal pigment epithelium (RPE)[1] that depends on interphotoreceptor retinoid binding protein (IRBP). Apo-IRBP is much more effective in promoting the release of 11-*cis*-retinal from the RPE than the apo forms of other retinoid binding proteins (*5*). In addition, apo-IRBP is only effective when it is present on the apical, but not basal, side of the RPE (*6*). Another finding that challenges the assumptions about random diffusion is the identification of an ATP-dependent transporter (ABCR or ABCA4) that transports all-*trans*-retinal released from bleached rhodopsin across membranes (*7*−*9*). Mutations in ABCR cause a wide spectrum of human vision diseases from retinitis pigmentosa to macular degeneration. Prior to the surprising discovery of ABCR's role in retinoid transport, there was no biochemical or physiological evidence for the existence of such a transporter.

Retinol is the main transport form of vitamin A in the blood. Although free retinol can also diffuse through membranes, it seldom exists in its free form. Retinol binding protein (RBP) is the specific carrier of vitamin A in the blood (*10, 11*). During transport in the blood, virtually all retinol is bound to RBP. RBP solubilizes retinol, and the retinol−RBP complex cannot freely diffuse through the membrane. Unlike ABCR, which was not predicted to exist, evidence has accumulated for more than 30 years for the existence of a membrane receptor for RBP that mediates cellular vitamin A uptake (*12*−*25*). Using an unbiased strategy, the membrane receptor for RBP has been identified as a multitransmembrane domain protein STRA6. STRA6 binds to RBP with high affinity and mediates cellular uptake of vitamin A from the retinol−RBP complex (holo-RBP) (*26*). STRA6 represents a rare example of a eukaryotic membrane transport system that depends on an extracellular carrier protein but does not rely on endocytosis. Consistent with the essential roles of vitamin A in human development, mutations in human STRA6 cause severe pathological phenotypes such as anophthalmia, mental retardation, congenital heart defects, and lung hyperplasia (*27, 28*).

Since STRA6 is a novel membrane transport protein not homologous to any other proteins with known function, one difficulty in studying STRA6's structure and function is that it has no obvious functional domains (e.g., ATP binding

[†] This project was supported by National Institutes of Health Grant 1R01EY018144 (H.S.).

* To whom correspondence should be addressed: Department of Physiology, 53-231 CHS, 650 Charles E. Young Drive South, Los Angeles, CA 90095. Phone: (310) 206-4017. Fax: (310) 206-5661. E-mail: hsun@mednet.ucla.edu.

[‡] Department of Physiology.

[§] Jules Stein Eye Institute.

[||] Brain Research Institute.

[1] Abbreviations: RBP, retinol binding protein; holo-RBP, retinol−RBP complex; STRA6, stimulated by retinoic acid gene 6; LRAT, lecithin retinol acyltransferase; RPE, retinal pigment epithelium.

10.1021/bi8002082 CCC: $40.75
Published on Web 04/18/2008

domain). The transmembrane topology of STRA6 has never been studied experimentally. At the basic level, it is not even known which terminus of STRA6 faces the outside or inside of the cell. Determining the transmembrane topology of STRA6 is critically important in understanding its detailed molecular mechanism. The transmembrane topology of a membrane protein contains information regarding extracellular domains, transmembrane domains, and intracellular domains. For example, the membrane topology of a channel is essential for elucidation of functional domains within it, such as the ligand binding region and the pore.

Common methods of determining the transmembrane topology of membrane proteins on the cell surface include epitope tagging (*29, 30*) and cysteine modification (*31*). Because STRA6 has a large number of cysteine residues (14 for bovine STRA6), mutating all cysteine residues to create the cysteine-less protein is likely to have a large impact on the protein's structure and function. We therefore chose epitope tagging as the primary method of elucidation of STRA6's transmembrane topology. This technique takes advantage of the fact that STRA6's natural cellular location is the plasma membrane (*32, 33*), which allows interaction with RBP, its ligand outside the cell. As a secondary method, we used a lysine accessibility technique to study a region of STRA6 not resolved by the epitope tagging method.

EXPERIMENTAL PROCEDURES

Myc Tagging. All experiments in this study were performed on bovine STRA6. For insertions of Myc into different regions of STRA6, an *Eco*RI and *Bam*HI linker was engineered into distinct sites in STRA6 cDNA by PCR. For Myc-tagged proteins M1−M13, the linker was inserted between the following pairs of residues: 16 and 17, 84 and 85, 133 and 134, 170 and 171, 197 and 198, 272 and 273, 323 and 324, 357 and 358, 407 and 408, 461 and 462, 509 and 510, 548 and 549, and 593 and 594, respectively. For M14, the linker was appended to the C-terminus. Two linker oligos that have *Eco*RI and *Bam*HI sites at each end and encode the Myc sequence (EQKLISEEDLN) flanked by three glycines were inserted into these engineered *Eco*RI and *Bam*HI sites (the *Eco*RI and *Bam*HI sites used in the cloning encode amino acids EF and GS, respectively). All final constructs were sequenced to rule out spurious mutations.

Cell Transfection. COS-1 cells or HEK293 cells were transfected using FuGENE 6 transfection reagent (Roche). All assays and harvesting of cells were performed 24−30 h after transfection. All assays based on live cells were conducted with COS-1 cells because of their strong attachment to the culture dish during washes. These studies include cell-surface protein quantitation studies, vitamin A uptake assays, and RBP binding assays. Since the transfection efficiency is higher for HEK293 cells than COS-1 cells, HEK293 cells were used for localization studies since these protocols are based on fixed cells instead of live cells.

Live Cell Staining and Permeabilized Cell Staining. STRA6−Myc constructs were transfected into HEK293 cells growing on gelatin-coated coverslips. Twenty-four hours after transfection, purified anti-Myc monoclonal antibody was added to the medium at a concentration of 2 μg/mL. After incubation for 1 h at 37 °C, the cells were washed with Hank's buffered salt solution (HBSS) three times and fixed in 4% paraformaldehyde in phosphate-buffered saline (PBS) for 10 min at room temperature. After three washes with PBS, the fixed cells were incubated with blocking buffer (5% normal goat serum and 0.3% Triton X-100 in PBS) for 1 h at room temperature. The cells were then incubated with Alexa Fluor 488-conjugated goat anti-mouse antibody (Molecular Probes) diluted in blocking buffer for an additional 1 h at room temperature. After three washes with PBS, the coverslips containing cells were mounted onto slides using VectaShield mounting medium (Vector Laboratories). The cell-surface expression of STRA6−Myc proteins was examined by fluorescence microscopy. Live cell staining for Rim-tagged STRA6 proteins was performed identically as described above except that anti-Rim tag monoclonal antibody (Rim3F4) was used. Permeabilized staining was performed using live cell staining procedures except that cells were incubated with the primary antibody after they had been fixed. Briefly, 24 h after transfection, cells were fixed in 4% paraformaldehyde in PBS for 10 min at room temperature. After three washes with PBS, the cells were incubated with blocking buffer for 1 h. All subsequent procedures were identical as described above for live cell staining.

Quantitation of Cell-Surface Expression. For quantitation of cell-surface expression, COS-1 cells were transfected with STRA6−Myc constructs. Twenty-four hours after transfection, purified anti-Myc monoclonal antibody was added to the medium at a concentration of 2 μg/mL for 1 h. After three washes with HBSS, the cells were incubated in 5% normal rabbit serum in serum free medium (SFM) for 15 min. Rabbit anti-mouse antibody conjugated to alkaline phosphatase diluted 1:4000 in 5% normal rabbit serum in SFM was then added to the cells and incubated for 1 h at 37 °C. After four washes with HBSS, cells were lysed in 1% Triton X-100 in PBS with protease inhibitors. Insoluble materials were removed by centrifugation at 16000*g* for 5 min at 4 °C. Alkaline phosphatase (AP) activity in the supernatant was measured using pNPP (Sigma). Quantitation of cell-surface expression for Rim-tagged STRA6 proteins was performed similarly as described above except that anti-Rim tag monoclonal antibody (Rim3F4) was used.

Vitamin A Uptake Assay. Production of the [^{3}H]retinol−RBP complex and uptake of cellular [^{3}H]retinol from the [^{3}H]retinol−RBP complex were performed similarly as described previously (*26*). All STRA6 variants were cotransfected with lecithin retinol acyltransferase (LRAT) for the vitamin A uptake assay. COS-1 cells express very low or undetectable levels of LRAT. Briefly, cells were washed with HBSS before incubation with the [^{3}H]retinol−RBP complex diluted in serum free medium (SFM) for 1 h at 37 °C. The reactions were stopped by removing the medium, washing the cells with HBSS, and solubilizing the cells in 1% Triton X-100 in PBS. Radioactivity was measured with a scintillation counter.

RBP Binding Assay. Quantitation of RBP binding to STRA6 was performed similarly as described using an alkaline phosphatase−RBP fusion protein (AP−RBP) (*26*). We have shown previously that AP tagged at the N-terminus of RBP does not interfere with RBP's interaction with either the RBP receptor in native cells or expressed STRA6 (*26*). Briefly, transfected cells grown on 12-well cell culture plates were washed once with HBSS and incubated with AP−RBP diluted in SFM at 37 °C for 1 h. The reaction was stopped

by washing cells twice with HBSS. The cells were then lysed in 200 μL of cold PBS containing 1% Triton X-100 and protease inhibitors per well. The cell lysates were centrifuged at 3000*g* and 4 °C for 5 min. The supernatants were removed and heated at 65 °C for 1 h. Twenty microliters of the heated lysate was mixed with 200 μL of pNPP (Sigma) and incubated at 37 °C for 1 h for the AP color reaction. The reactions were stopped by adding 50 μL of 3 M NaOH, and the mixtures were transferred to a 96-well plate for reading in a microplate reader at 405 nm.

Cell-Surface Biotinylation of STRA6. For cell-surface biotinylation of STRA6, HEK293 cells transfected with STRA6 constructs for 24 h were washed once with PBS before being harvested in PBS with 5 mM EDTA. The cells were further washed with PBS three times to remove serum proteins after being harvested by gentle pelletting at 3000 rpm for 30 s using an Eppendorf 5417C centrifuge. Immediately before use, 2 mg of NHS-PEO_4-Biotin (Pierce) was dissolved in 170 μL of water. Then 30 μL of the biotin solution was added to 1 mL of cells suspended in PBS. After the mixture had been rotated at room temperature for 30 min, the biotinylation reaction was stopped by washing cells with PBS with 100 mM glycine. Since a large number of cell-surface proteins can be biotinylated, biotinylated STRA6 needs to be purified for the specific detection of its biotinylation. We inserted a 6xHis tag and a Rim tag (*8*) into a loop region of STRA6 (the M10 position in Figure 1), which is well exposed in native STRA6 (Figure 3). These two tags allow tandem-affinity purification of STRA6 from crude cellular membranes.

Tandem-Affinity Purification of STRA6. Tandem-affinity purification of 6xHis-Rim-tagged STRA6 was achieved by purification of a 6xHis tag followed by purification of the Rim tag using a previously described protocol with modifications (*8, 34*). All procedures were performed on ice or at 4 °C. Briefly, after cell-surface biotinylation of cells expressing wild-type or mutant 6xHis-Rim-STRA6 (one 10 cm dish per construct), crude cellular membranes were prepared and suspended in 50 μL of PBS containing protease inhibitors. Cell membranes were then solubilized with 1 volume of 1% dodecyl maltoside and 20% glycerol in PBS and quickly diluted by addition of 8 volumes of dilution solution (PBS containing 0.75% CHAPS, 10% glycerol, 1 mg/mL brain polar lipid, 2 mM β-mercaptoethanol, and protease inhibitors). The mixture was incubated for 30 min on ice, and insoluble material was removed by centrifugation at 16000*g* for 5 min. The soluble fraction was incubated in 50 μL of a slurry of TALON resin (Clontech) overnight in the presence of 5 mM imidazole. The resin was then washed three times with wash solution (PBS containing 0.75% CHAPS, 1 mg/mL brain polar lipid, and 10 mM imidazole). 6xHis-Rim-STRA6 was eluted in 0.75% CHAPS, 1 mg/mL brain polar lipid, and 100 mM imidazole in PBS. The eluted material was incubated for 3 h with Rim3F4 antibody conjugated to Sepharose beads. Sepharose beads were then washed quickly three times with 1% CHAPS and 1 mg/mL brain polar lipid in PBS. The beads were washed once more with 0.2% CHAPS, 1 mg/mL brain polar lipid in PBS by incubating for 15 min. Finally, 6xHis-Rim-STRA6 was eluted in 80 μl of 0.2% CHAPS, 1 mg/ml brain polar lipid, and 0.5 mg/mL Rim3F4 peptide in PBS (incubation time of 40 min). Biotinylated STRA6 in the eluted material was detected by Western blot analysis using Streptavidin-HRP (Pierce) to detect biotin.

RESULTS

STRA6 is a largely hydrophobic protein, as indicated by its amino acid composition and its hydropathy profile (Figure 1). Two computer programs designed to predict transmembrane topology (SOSUI and TMPRED) both predict 11 transmembrane domains for STRA6 (Figure 1). However, computer-predicted topology is often different from real topology. Since STRA6 is localized to the plasma membrane, its topology can be determined on the basis of the accessibility of each region of STRA6 to the extracellular space. This is most commonly achieved by epitope tagging. We inserted the Myc tag into the 14 hydrophilic regions of bovine STRA6 (STRA6−Myc), including the N-terminal, C-terminal, and all putative intracellular and extracellular loop regions (Figure 1). The least conserved regions were chosen for each insertion. These constructs are named STRA6-M1−STRA6-M14.

Only when a Myc tag is exposed to the extracellular face of STRA6 can an anti-Myc antibody bind to the tag in live cells. Therefore, positive anti-Myc staining of live cells indicates that the Myc tag is localized to the extracellular region of STRA6. When a Myc tag is inserted into a hydrophilic region but cannot be stained by anti-Myc antibody in live cells, it is likely localized intracellularly. Alternatively, negative anti-Myc staining of live cells may be due to the inaccessibility of the Myc epitope even if it is on the cell surface or the complete absence of STRA6 protein due to the Myc insertion. For these reasons, we need to perform the control experiments consisting of using anti-Myc antibody to stain permeabilized cells to make sure that STRA6 can still be detected in permeabilized cells. A third possibility for the lack of live cell-surface staining by anti-Myc antibody is that the Myc insertion causes misfolding of STRA6 and prevents its proper expression on the cell surface. For this reason, we need to perform functional analysis of STRA6−Myc proteins, including a live cell RBP binding assay and live cell vitamin A uptake assay from holo-RBP. These STRA6-dependent functional assays will test whether the STRA6−Myc proteins are functionally expressed on the cell surface.

In addition to determining the transmembrane topology of STRA6, these STRA6−Myc proteins may also help to reveal the role of each hydrophilic region in STRA6's biochemical activity, including RBP binding and vitamin A uptake. For example, if a STRA6−Myc protein is expressed on the cell surface, as assayed by live cell anti-Myc staining, but has a reduced level of RBP binding, the region of STRA6 where the Myc tag is inserted is likely involved in RBP binding.

Live Cell and Permeabilized Cell Staining. The STRA6−Myc constructs were transfected into HEK293 cells. Anti-Myc immunostaining of live transfected cells revealed that cells transfected with STRA6-M1, STRA6-M3, STRA6-M5, and STRA6-M10 have the Myc epitope exposed on the cell surface of live cells, but cells transfected with the other 10 constructs do not (Figure 2). To confirm that the 10 negative STRA6−Myc constructs are expressing the protein, we performed anti-Myc immunostaining of fixed and perme-

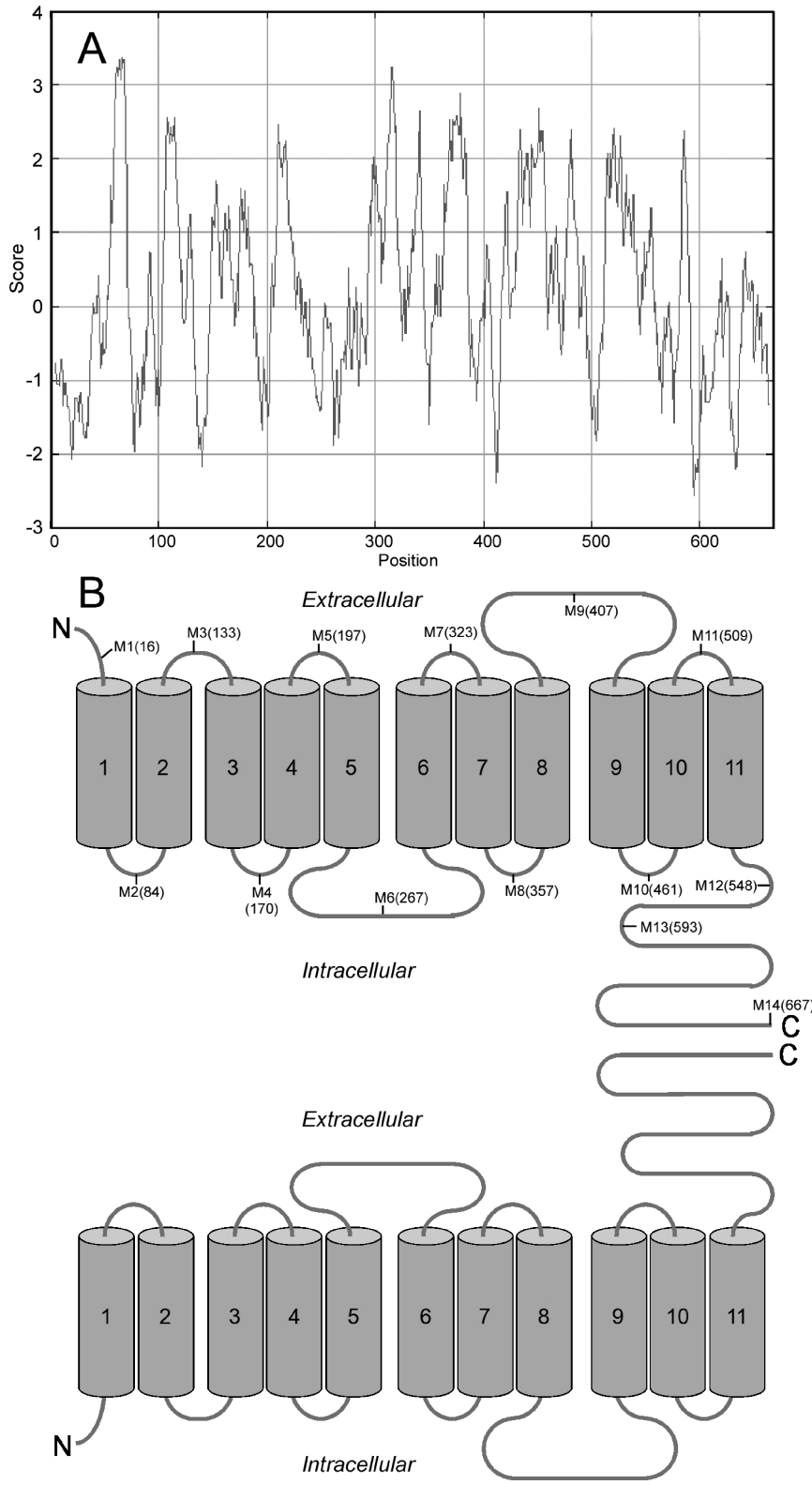

FIGURE 1: Hydropathy plot of STRA6 and locations of Myc insertions. (A) Kyle−Doolittle hydropathy plot for bovine STRA6. Positive scores indicate hydrophobicity and negative scores hydrophilicity. (B) Two computer programs for transmembrane domain prediction, SUSUI and TMPRED, predicted 11 transmembrane domains for bovine STRA6, although they cannot distinguish the two possible orientations. The locations of the Myc insertions are indicated in the first transmembrane topology model. The number in parentheses indicates the residue after which the Myc tag was inserted.

abilized cells as a control for the proper expression of the tagged STRA6 (Figure 2). All STRA6−Myc constructs expressed the Myc-tagged STRA6 (Figure 2). This indicates that all Myc epitopes in the STRA6−Myc proteins were accessible and not hidden within the protein. Although 10 STRA6−Myc constructs are negative for live cell staining, their fixed and permeabilized staining signals are similar to those positive for live cell staining. We further quantitated the anti-Myc antibody binding using an alkaline phosphatase-tagged secondary antibody (Figure 3). This quantitation con-

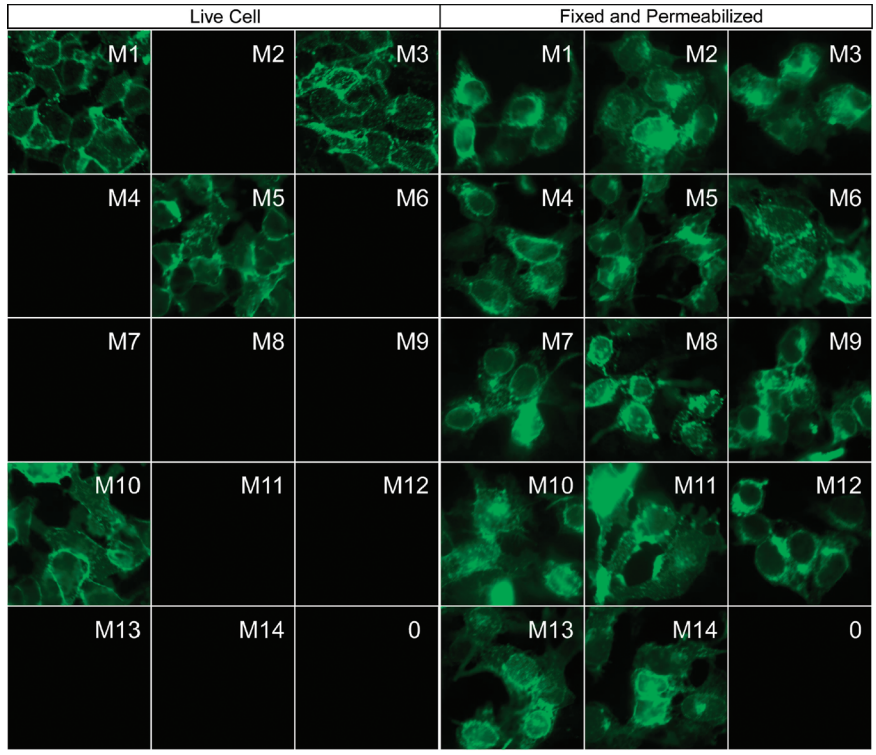

FIGURE 2: Anti-Myc live cell staining and anti-Myc permeabilized staining of STRA6−Myc proteins. HEK293 cells transfected with STRA6−Myc constructs were either stained with anti-Myc antibody in live cells (left panel) or stained with anti-Myc antibody after the cells had been fixed and permeabilized. Anti-mouse Alexa Fluor 488 (green signal) was used as a secondary antibody. Untransfected cells are labeled as "0".

firmed the anti-Myc live cell staining data (M1, M3, M5, and M10 are on the extracellular side) and also identified STRA6-M10 as the construct with the strongest signal for Myc expression on the cell surface.

Vitamin A Uptake and RBP Binding Activity of the STRA6−Myc Proteins. To further characterize these proteins, we compared the vitamin A uptake activities of 14 Myc-tagged STRA6 constructs with that of wild-type STRA6. Although 10 STRA6−Myc constructs do not express the Myc epitope on cell surface, seven of them have significant vitamin A uptake activity from holo-RBP (Figure 4). Their vitamin A uptake activities from extracellular holo-RBP suggest that these proteins are functional and are expressed on the cell surface. Combined with their positive staining of permeabilized cells, these results suggest that the absence of Myc staining in live cells of these proteins is due to the intracellular localization of the Myc epitope. In contrast, STRA6-M7, STRA6-M8, and STRA6-M12 have little uptake activity (Figure 4). Since these three constructs do not have the Myc epitope expressed on the cell surface, the most likely explanation for both the absence of the Myc epitope and vitamin A uptake activity is protein misfolding that results in nonfunctional STRA6. Therefore, M7, M8, and M12 are not informative in determining the intracellular and extracellular locations of these positions.

We also tested the RBP binding abilities of STRA6-M1−STRA6-M14 proteins with wild-type STRA6 (Figure 5). As in the vitamin A uptake assay, STRA6-M2, STRA6-M4, STRA6-M6, STRA6-M9, STRA6-M11, STRA6-M13, and STRA6-M14 had significant RBP binding activity, indicating the proper expression of these proteins on the cell surface. The absence of the Myc epitope on their cell surface is due to the localization of the epitope on intracellular domains. As in the vitamin A uptake assay, STRA6-M7, STRA6-M8, and STRA6-M12 have dramatically reduced RBP binding activity compared to wild-type STRA6. In addition, STRA6-M5 and STRA6-M10 also have significantly reduced RBP binding activity. Since STRA6-M5 and STRA6-M10 are expressed well on the cell surface (Figures 2 and 3), this result suggests that insertion of Myc at these extracellular positions likely interferes with the binding of RBP to STRA6. The relative vitamin A uptake activity of each STRA6−Myc protein compared to that of wild-type STRA6 is not always identical to the RBP binding activity. This difference may be explained by the distinct nature of these assays. The vitamin A uptake activity represents the cumulative activity of vitamin A uptake over a period of time (i.e., 1 h), whereas the RBP binding activity represents steady state binding of RBP at a single time point. A related fact is that RBP's binding to its receptor STRA6 is transient (data not shown). This transient nature is important for RBP's delivery of vitamin A to cells because the uptake cannot continue if RBP fails to leave STRA6 after retinol uptake. Because uptake of retinol from holo-RBP depends on both the binding of RBP and the turnover of RBP from STRA6, the steady state RBP binding activity of a STRA6−Myc mutant may not always predict its accumulated vitamin A uptake activity.

Lysine Accessibility in Live Cells as a Method of Revealing Cell-Surface-Exposed Lysines. Of the three positions whose intra- or extracellular locations were not revealed by STRA6−Myc proteins (M7, M8, and M12), position M12 is likely intracellular on the basis of the properties of its adjacent regions. Because positions M11, M13, and M14 are all intracellular and there are too many hydrophilic residues between M12 and M13 for this region to have a transmem-

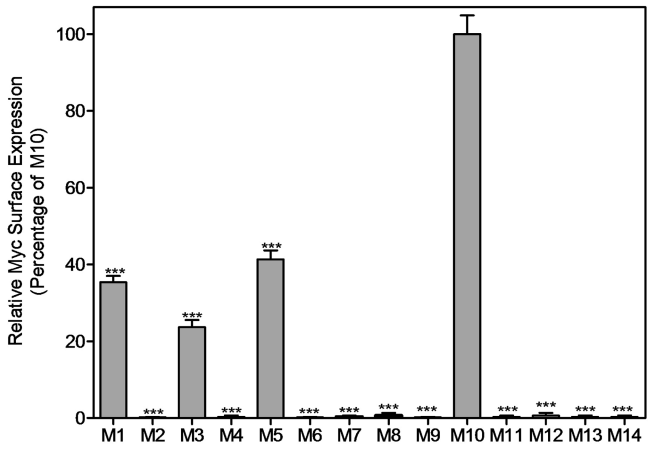

FIGURE 3: Quantitation of cell-surface expression of STRA6−Myc series. To quantitate the Myc epitope exposed to the cell surface for different STRA6−Myc proteins, anti-mouse alkaline phosphatase was used as the secondary antibody after the anti-Myc antibody was bound to the cell surface on live cells. The activity of alkaline phosphatase bound to cells was quantitated. Activity of STRA6-M10, which has the highest activity, is defined as 100%. The statistical significance of cell-surface expression levels was determined against that of M10 with a Student's *t* test (three asterisks, $P < 0.001$).

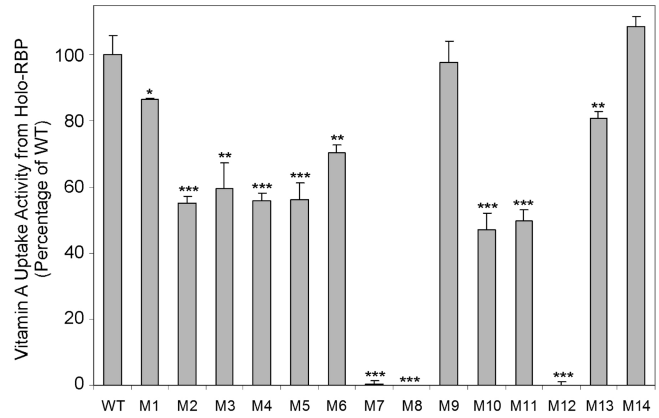

FIGURE 4: Vitamin A uptake activities from holo-RBP of the STRA6−Myc series. All STRA6 variants were cotransfected with LRAT into COS-1 cells for the vitamin A uptake assay. For the vitamin A uptake assay, the [^{3}H]retinol−RBP complex was added to cells. After incubation for 1 h, cells were washed with PBS, and total radioactivity from cell lysate was determined as uptake activity. Activity of wild-type STRA6 is defined as 100%. The statistical significance of vitamin A uptake activity was determined against the activity of wild-type STRA6 with a Student's *t* test (one asterisk, $P < 0.05$; two asterisks, $P < 0.01$; three asterisks, $P < 0.001$).

brane domain, M12 is also likely intracellular. Another piece of indirect evidence for localizing M12 intracellularly is the presence of a nonconserved cysteine between M12 and M13. If M12 were extracellular, this cysteine located in the hydrophilic region immediately following M12 should also be extracellular. However, extracellular cysteines in proteins tend to be extremely conserved because they are oxidized to form disulfide bonds. Although unlikely, we cannot completely rule out the possibility that M12 is extracellular.

We designed an independent method of determining the locations of M7 and M8. We noticed two lysine residues (positions 325 and 357) located immediately adjacent to the M7 and M8 insertion sites. Because only two other lysine residues (positions 200 and 203, located near M5) are located in regions potentially exposed to the extracellular space, the accessibility of these lysine residues to membrane impermeable biotinylation reagent in live cells may help to determine their possible extracellular location. For this assay, we used the membrane impermeable biotinylation reagent NHS-PEO_4-Biotin (Pierce), which reacts with lysine residues. Since a large number of cell-surface membrane proteins can potentially be biotinylated, we used tandem-affinity purification to isolate STRA6 after cell-surface biotinylation of live cells. We first created three STRA6 mutants (K200A/K203A/K325A/K357A, K200A/K203A, and K325A/K357A). Cell-surface biotinylation followed by tandem-affinity purification of the wild type and the three STRA6 mutants showed that wild-type STRA6 and mutant K200A/K203A can be biotinylated in live cells, whereas mutants K200A/K203A/K325A/K357A and K325A/K357A exhibited no detectable biotinylation in live cells (Figure 6A). Western blots for the STRA6 protein detected successful purification of all STRA6 variants by tandem-affinity purification. This result narrows down the major exposed lysine residue(s) in live cell to residues 325 and 357, which are located between M7 and M8. We further created STRA6 mutants K325A and K357A and found that lysine 357 is the major lysine residue responsible for STRA6 biotinylation in live cells (Figure 6B). Because the K357A mutant is expressed well on the cell surface (Figure 6D), loss of biotinylation in the K357A mutant is due to the loss of the extracellularly accessible lysine. As residue 357 is immediately adjacent to position M8, this result suggests that M8 is extracellular.

There are other pieces of evidence suggesting the extracellular location of the region between M7 and M8. In an independent study of more than 900 random STRA6 mutants, we identified an essential RBP binding domain in the region of STRA6 located between M7 and M8 (unpublished result). This result suggests that the seventh "transmembrane domain" in the computer-predicted model (Figure 1) is actually an extracellular domain. Consistently, this domain is the only computer-predicted transmembrane domain that has a significant number of hydrophilic amino acids. In bovine STRA6, four hydrophilic residues are located in this domain, including aspartate, glutamate, and arginine residues. Interestingly, the equivalent region in mouse STRA6 is not predicted to be a transmembrane domain by the computer programs. The extracellular location of this domain (residues between M7 and M8) is also consistent with the intracellular location of M6 and M9, and the sixth and eighth transmembrane domains (Figure 1B) which are completely devoid of hydrophilic residues. The inaccessibility of the biotinylation reagent NHS-PEO_4-Biotin to lysine 325 is likely due to its location in a protein domain that prevents efficient access by the biotinylation reagent. Interestingly, lysine 325 is located immediately adjacent to a transmembrane domain (it is the first hydrophilic residue after a transmembrane domain).

STRA6 Topology Model. The results of the epitope tagging experiments are summarized in Figure 7. The 14 Myc-tagged STRA6 proteins can be categorized into four groups. Group 1 (STRA6-M1 and STRA6-M3) has the Myc epitope expressed on the cell surface and has significant vitamin A uptake activity and RBP binding activity. For group 1, the Myc epitope is inserted into the extracellular regions of STRA6, but the insertion does not substantially affect the interaction of RBP and STRA6 on the extracellular side.

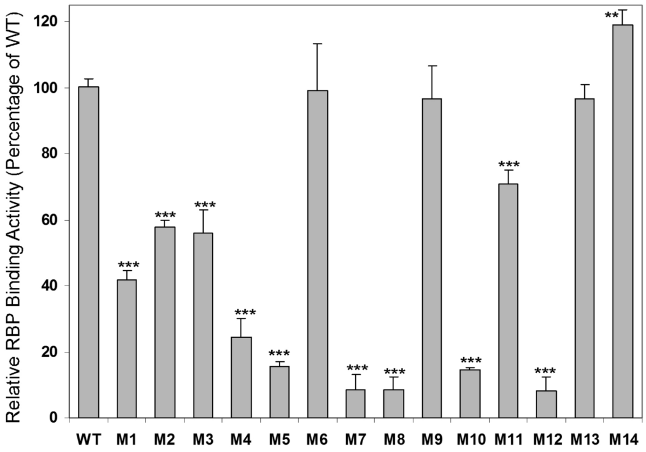

FIGURE 5: RBP binding activities of the STRA6−Myc series. To measure RBP binding activity, AP−RBP was added to COS-1 cells transfected with the STRA6−Myc constructs for 1 h. After unbound AP−RBP was washed off with PBS, alkaline phosphatase activity associated with the cells was measured by color reaction using pNPP as the substrate. Activity of wild-type STRA6 is defined as 100%. The statistical significance of RBP binding activity was determined against the activity of wild-type STRA6 with a Student's *t* test (two asterisks, $P < 0.01$; three asterisks, $P < 0.001$).

Group 2 (STRA6-M5 and STRA6-M10) also has the Myc epitope expressed on the cell surface but shows a strong reduction in RBP binding activity. This is even more evident given the fact that they are better expressed on the cell surface than STRA6-M1 and STRA6-M3 (Figure 3). For group 2, the Myc epitope is also inserted into the extracellular regions of STRA6, but these extracellular regions likely contribute to the interaction of STRA6 with RBP. Group 3 (STRA6-M2, STRA6-M4, STRA6-M6, STRA6-M9, STRA6-M11, STRA6-M13, and STRA6-M14) does not have the Myc epitope expressed extracellularly and has significant vitamin A uptake activity and RBP binding activity. For group 3, the absence of anti-Myc antibody binding in live cells is due to the insertion of the epitope on the intracellular regions of STRA6, because these proteins are still expressed on the cell surface and anti-Myc antibody can stain the permeabilized cells. Group 4 (STRA6-M7, STRA6-M8, and STRA6-M12) also does not have the Myc epitope expressed extracellularly but has no vitamin A uptake activity or RBP binding activity. For group 4, the absence of extracellular localization of the Myc epitope is due to the absence of surface expression of these proteins. A transmembrane topology model for STRA6 (Figure 7) is proposed on the basis of these experiments, the lysine accessibility experiment (Figure 6), and the logic that a transmembrane domain is flanked by an extracellular domain and an intracellular domain.

Functional Effects of the Loss of Extracellular Cysteines in STRA6. There are two extracellular cysteines (residues 44 and 195 of bovine STRA6) in the STRA6 topology model (Figure 7). These cysteines are highly conserved. We tested the effect of mutating these two cysteines to alanines on STRA6's functions (Figure 8). We found that the C44A and C195A mutants have significant losses of vitamin A uptake activities from holo-RBP (Figure 8A) and RBP binding activities (Figure 8B). However, their cell-surface expression levels are similar to that of wild-type STRA6 (Figure 8C,D). These results suggest that the loss of RBP binding, instead of the loss of cell-surface expression, is largely responsible

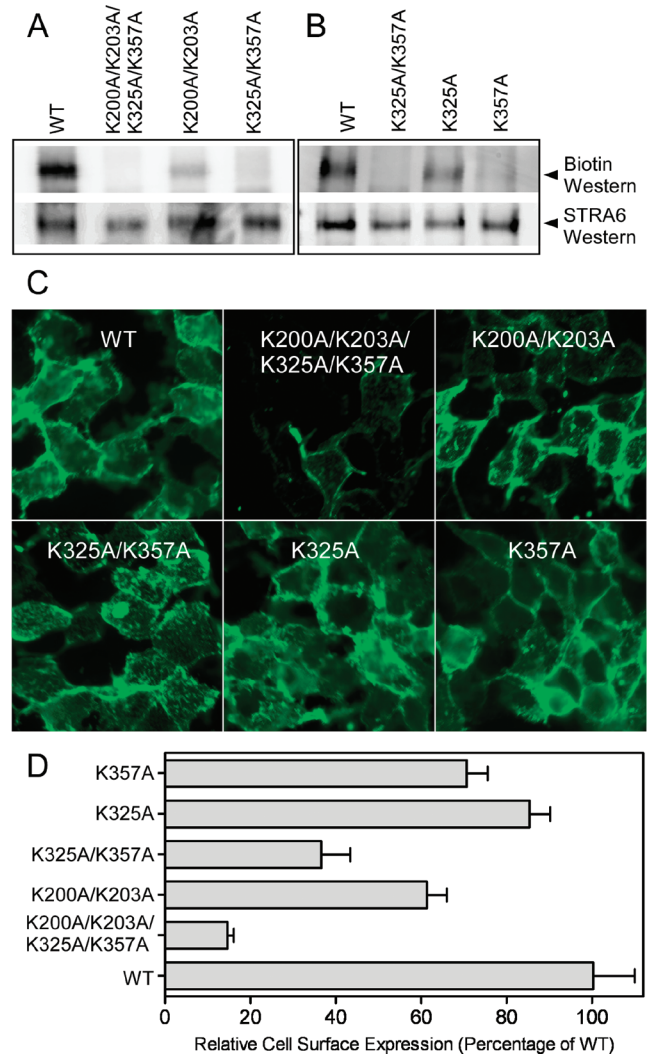

FIGURE 6: Cell-surface biotinylation of STRA6 and identification of STRA6 mutants resistant to biotinylation. For tandem-affinity purification and cell-surface expression quantitation of STRA6, all STRA6 variants in this figure are tagged with a 6xHis tag and a Rim tag in an extracellular loop of bovine STRA6 (between residues 133 and 134). (A) Western blots detecting biotin (top panel) and STRA6 (bottom panel) after tandem-affinity purification of cell-surface-biotinylated wild-type STRA6 and STRA6 mutants K200A/K203A/K325A/K357A, K200A/K203A, and K325A/K357A. (B) Western blots detecting biotin (top panel) and STRA6 (bottom panel) after tandem-affinity purification of cell-surface-biotinylated wild-type STRA6 and STRA6 mutants K325A/K357A, K325A, and K357A. (C) Live cell staining of STRA6 variants included in the biotinylation study. (D) Quantitation of cell-surface expression for wild-type STRA6 and STRA6 mutants K200A/K203A/K325A/K357A, K200A/K203A, K325A/K357A, K325A, and K357A using Rim3F4 monoclonal antibody. The expression level of wild-type STRA6 is defined as 100%.

for the loss of vitamin A uptake activity for these mutants. Since RBP is an extracellular ligand of STRA6, the effects of these mutations on RBP binding are consistent with the extracellular locations of these two cysteine residues.

DISCUSSION

STRA6 functions both as a membrane receptor for RBP and as a transport protein that mediates cellular uptake of vitamin A from holo-RBP. In this paper, we determined STRA6's transmembrane topology, which is a fundamental aspect of the structural information for a multitransmembrane

STRA6 Constructs	Live Cell Staining	Permeabilized Cell Staining	Retinol Uptake Activity [%±SD of WT]	Surface Expression Quantitation [%±SD of M10]	RBP Binding Activity [%±SD of WT]	Category
M1	+	+	86.43±5.97	35.33±2.88	41.67±2.87	1
M2	−	+	55.07±2.00	0.17±0.29	57.87±1.97	3
M3	+	+	59.40±7.96	23.67±3.22	56.00±7.00	1
M4	−	+	55.68±2.59	0.43±0.59	24.32±5.94	3
M5	+	+	56.21±4.85	41.33±4.04	15.66±1.32	2
M6	−	+	70.25±2.58	0.13±0.35	99.31±14.00	3
M7	−	+	0.39±1.08	0.40±0.53	8.47±4.48	4
M8	−	+	0.00±0.624	0.77±1.08	8.53±4.01	4
M9	−	+	97.90±6.44	0.23±0.25	96.51±10.16	3
M10	+	+	47.15±4.96	100±8.43	14.43±0.90	2
M11	−	+	49.59±3.56	0.43±0.49	70.75±4.28	3
M12	−	+	0.00±1.87	0.73±1.02	8.08±4.24	4
M13	−	+	80.76±2.27	0.33±0.58	96.51±4.53	3
M14	−	+	108.41±3.19	0.27±0.29	119.00±4.58	3

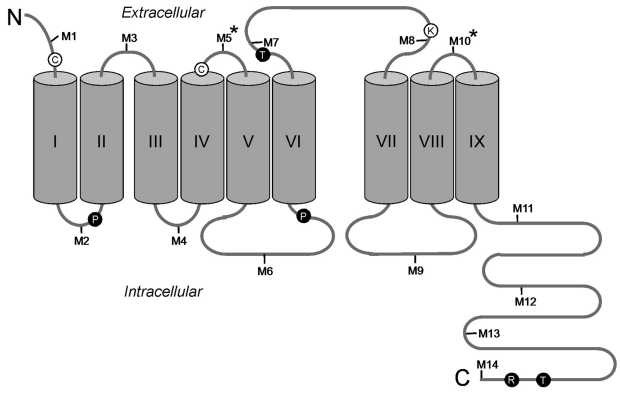

FIGURE 7: Transmembrane topology model of STRA6. A summary (top panel) of the properties of the STRA6−Myc proteins. In the second and third columns, a plus sign indicates positive staining and a minus sign indicates negative staining. A model (bottom panel) for the transmembrane topology of STRA6. Locations of the Myc epitopes are indicated. The Myc epitopes that were on the extracellular side and substantially reduced STRA6's level of RBP binding are marked with asterisks. The lysine residue in STRA6 shown by live cell biotinylation to be exposed on the cell surface is also shown. The two extracellular cysteines (residues 44 and 195 of bovine STRA6) are also noted. Missense mutations in STRA6 associated with human birth defects (*27*) are indicated as black circles with white letters. These mutations are P90(91)L, P293(294)L, T321(322)P, T644(643)M, and R655(654)C (numbers in parentheses are amino acid residues in bovine STRA6).

domain protein. Compared with one orientation (extracellular N-terminus) of the computer-predicted model (Figure 1), our experimentally confirmed model is similar to the predictions in the N-terminal half of the protein. Our topology model suggests that STRA6 has 19 distinct domains, including five extracellular domains, nine transmembrane domains, and five intracellular domains (Figure 7). Many membrane transporters have 8−12 transmembrane domains (*35*). Although STRA6 represents a new membrane transport protein not homologous to any protein of known function, its number of transmembrane domains lies within this range. Most, if not all, proteins with more than seven transmembrane domains function as membrane transporters or channels. A large number of transmembrane membrane domains potentially makes it more feasible to form a specific transmembrane pore, through which the ligand of the transporter or channel can pass.

In addition to epitope tagging and lysine accessibility, the locations of cysteine residues also support this topology

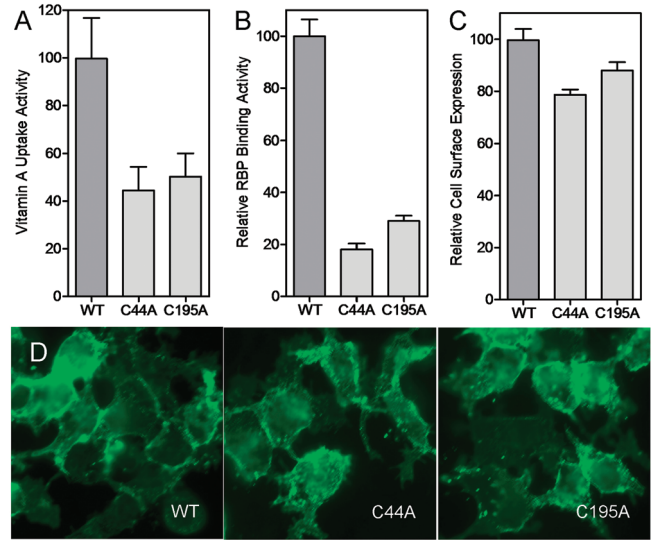

FIGURE 8: Comparison of wild-type STRA6 and C44A and C195A mutants. For live cell staining and cell-surface expression quantitation of STRA6, all STRA6 variants in this figure are tagged with a Myc tag on an extracellular loop of bovine STRA6 (between residues 133 and 134). (A) [^{3}H]Retinol uptake activity from [^{3}H]retinol−RBP. (B) AP−RBP binding activity. (C) Quantitation of cell-surface expression. (D) Live cell staining using anti-Myc antibody. For panels A−C, the activity of wild-type STRA6 is defined as 100%.

model. There are only two cysteine residues located extracellularly in the topology model (Figure 7). Consistent with the importance of extracellular cysteines in the stabilization of protein structure through disulfide bonds, this pair of cysteines is absolutely conserved from *Xenopus* STRA6 to human STRA6. We have shown that a mutation in either of these two cysteines leads to a substantial loss of RBP binding activity, supporting the extracellular locations of these residues (Figure 8). Because of the unique biochemical properties and functions of cysteines, nonconserved cysteines are seldom, if ever, found in extracellular domains of eukaryotic proteins. Consistently, all three nonconserved cysteine residues in bovine STRA6 are located intracellularly in the topology model (one near M6, one near M9, and one near M12).

This study identified two regions (M5 and M10) of STRA6 that are likely to participate in the interaction of STRA6 and RBP. Although STRA6-M5 and STRA6-M10 are expressed well on the cell surface, they have substantially reduced RBP binding activity. This model also reveals a large C-terminal region of STRA6. In addition to the evidence presented in this study, there is an additional piece of evidence supporting the intracellular orientation of the C-terminal domain. A polyclonal antibody recognizing an epitope on the C-terminal domain cannot recognize STRA6 on live cells but can recognize STRA6 in permeabilized cells (data not shown). The C-terminal region of STRA6 is highly conserved among human, mouse, and bovine STRA6. Why does STRA6 need such a long intracellular C-terminal domain? It is likely involved in uptake of vitamin A into cells and/or in the cellular targeting of STRA6. STRA6 is specifically targeted to the basolateral membrane of the RPE (*26*), a location consistent with its role in uptake of vitamin A from holo-RBP in choroidal blood. In addition, two pathogenic missense mutations in human STRA6 associ-

ated with severe birth defects are located on the C-terminus (Figure 7).

The elucidation of the transmembrane topology of STRA6 lays the groundwork for understanding the structure and function of this novel receptor and membrane transport protein. The transmembrane topology model demarcates STRA6 into extracellular, intracellular, and transmembrane domains. This general demarcation is critically important for future studies aimed at understanding the roles of these regions in STRA6 function and in elucidating the structural basis of its function both as a high-affinity receptor for RBP and in the transport of vitamin A into cells.

REFERENCES

1. Ross, A. C., and Gardner, E. M. (1994) The function of vitamin A in cellular growth and differentiation, and its roles during pregnancy and lactation. *Adv. Exp. Med. Biol. 352*, 187–200.
2. Blomhoff, R. (1994) Overview of Vitamin A Metabolism and Function, in *Vitamin A in Health and Disease* (Blomhoff, R., Ed.) pp 1−35, Marcel Dekker, Inc., New York.
3. Mark, M., Ghyselinck, N. B., and Chambon, P. (2006) Function of retinoid nuclear receptors: Lessons from genetic and pharmacological dissections of the retinoic acid signaling pathway during mouse embryogenesis. *Annu. Rev. Pharmacol. Toxicol. 46*, 451–480.
4. Dew, S. E., and Ong, D. E. (1994) Specificity of the retinol transporter of the rat small intestine brush border. *Biochemistry 33*, 12340–12345.
5. Carlson, A., and Bok, D. (1992) Promotion of the release of 11-cis-retinal from cultured retinal pigment epithelium by interphotoreceptor retinoid-binding protein. *Biochemistry 31*, 9056–9062.
6. Carlson, A., and Bok, D. (1999) Polarity of 11-cis retinal release from cultured retinal pigment epithelium. *Invest. Ophthalmol. Visual Sci. 40*, 533–537.
7. Weng, J., Mata, N. L., Azarian, S. M., Tzekov, R. T., Birch, D. G., and Travis, G. H. (1999) Insights into the function of Rim protein in photoreceptors and etiology of Stargardt's disease from the phenotype in abcr knockout mice. *Cell 98*, 13–23.
8. Sun, H., Molday, R. S., and Nathans, J. (1999) Retinal stimulates ATP hydrolysis by purified and reconstituted ABCR, the photoreceptor-specific ATP-binding cassette transporter responsible for Stargardt disease. *J. Biol. Chem. 274*, 8269–8281.
9. Ahn, J., Wong, J. T., and Molday, R. S. (2000) The effect of lipid environment and retinoids on the ATPase activity of ABCR, the photoreceptor ABC transporter responsible for Stargardt macular dystrophy. *J. Biol. Chem. 275*, 20399–20405.
10. Newcomer, M. E., and Ong, D. E. (2000) Plasma retinol binding protein: Structure and function of the prototypic lipocalin. *Biochim. Biophys. Acta 1482*, 57–64.
11. Zanotti, G., and Berni, R. (2004) Plasma retinol-binding protein: Structure and interactions with retinol, retinoids, and transthyretin. *Vitam. Horm. 69*, 271–295.
12. Bok, D., and Heller, J. (1976) Transport of retinol from the blood to the retina: An autoradiographic study of the pigment epithelial cell surface receptor for plasma retinol-binding protein. *Exp. Eye Res. 22*, 395–402.
13. Chen, C. C., and Heller, J. (1977) Uptake of retinol and retinoic acid from serum retinol-binding protein by retinal pigment epithelial cells. *J. Biol. Chem. 252*, 5216–5221.
14. Rask, L., and Peterson, P. A. (1976) In vitro uptake of vitamin A from the retinol-binding plasma protein to mucosal epithelial cells from the monkey's small intestine. *J. Biol. Chem. 251*, 6360–6366.
15. Heller, J. (1975) Interactions of plasma retinol-binding protein with its receptor. Specific binding of bovine and human retinol-binding protein to pigment epithelium cells from bovine eyes. *J. Biol. Chem. 250*, 3613–3619.
16. Heller, J., and Bok, D. (1976) Transport of retinol from the blood to the retina: Involvement of high molecular weight lipoproteins as intracellular carriers. *Exp. Eye Res. 22*, 403–410.
17. Maraini, G., and Gozzoli, F. (1975) Binding of retinol to isolated retinal pigment epithelium in the presence and absence of retinol-binding protein. *Invest. Ophthalmol. 14*, 785–787.
18. Bhat, M. K., and Cama, H. R. (1979) Gonadal cell surface receptor for plasma retinol-binding protein. A method for its radioassay and studies on its level during spermatogenesis. *Biochim. Biophys. Acta 587*, 273–281.
19. Torma, H., and Vahlquist, A. (1984) Vitamin A uptake by human skin in vitro. *Arch. Dermatol. Res. 276*, 390–395.
20. Sivaprasadarao, A., and Findlay, J. B. (1988) The interaction of retinol-binding protein with its plasma-membrane receptor. *Biochem. J. 255*, 561–569.
21. Shingleton, J. L., Skinner, M. K., and Ong, D. E. (1989) Characteristics of retinol accumulation from serum retinol-binding protein by cultured Sertoli cells. *Biochemistry 28*, 9641–9647.
22. MacDonald, P. N., Bok, D., and Ong, D. E. (1990) Localization of cellular retinol-binding protein and retinol-binding protein in cells comprising the blood-brain barrier of rat and human. *Proc. Natl. Acad. Sci. U.S.A. 87*, 4265–4269.
23. Sivaprasadarao, A., and Findlay, J. B. (1994) Structure-function studies on human retinol-binding protein using site-directed mutagenesis. *Biochem. J. 300* (Part 2), 437–442.
24. Smeland, S., Bjerknes, T., Malaba, L., Eskild, W., Norum, K. R., and Blomhoff, R. (1995) Tissue distribution of the receptor for plasma retinol-binding protein. *Biochem. J. 305* (Part 2), 419–424.
25. Liden, M., and Eriksson, U. (2005) Development of a versatile reporter assay for studies of retinol uptake and metabolism in vivo. *Exp. Cell Res. 310*, 401–408.
26. Kawaguchi, R., Yu, J., Honda, J., Hu, J., Whitelegge, J., Ping, P., Wiita, P., Bok, D., and Sun, H. (2007) A membrane receptor for retinol binding protein mediates cellular uptake of vitamin A. *Science 315*, 820–825.
27. Pasutto, F., Sticht, H., Hammersen, G., Gillessen-Kaesbach, G., Fitzpatrick, D. R., Nurnberg, G., Brasch, F., Schirmer-Zimmermann, H., Tolmie, J. L., Chitayat, D., Houge, G., Fernandez-Martinez, L., Keating, S., Mortier, G., Hennekam, R. C., von der Wense, A., Slavotinek, A., Meinecke, P., Bitoun, P., Becker, C., Nurnberg, P., Reis, A., and Rauch, A. (2007) Mutations in STRA6 Cause a Broad Spectrum of Malformations Including Anophthalmia, Congenital Heart Defects, Diaphragmatic Hernia, Alveolar Capillary Dysplasia, Lung Hypoplasia, and Mental Retardation. *Am. J. Hum. Genet. 80*, 550–560.
28. Golzio, C., Martinovic-Bouriel, J., Thomas, S., Mougou-Zrelli, S., Grattagliano-Bessieres, B., Bonniere, M., Delahaye, S., Munnich, A., Encha-Razavi, F., Lyonnet, S., Vekemans, M., Attie-Bitach, T., and Etchevers, H. C. (2007) Matthew-Wood Syndrome Is Caused by Truncating Mutations in the Retinol-Binding Protein Receptor Gene STRA6. *Am. J. Hum. Genet. 80*, 1179–1187.
29. Borjigin, J., and Nathans, J. (1994) Insertional mutagenesis as a probe of rhodopsin's topography, stability, and activity. *J. Biol. Chem. 269*, 14715–14722.
30. Canfield, V. A., and Levenson, R. (1993) Transmembrane organization of the Na,K-ATPase determined by epitope addition. *Biochemistry 32*, 13782–13786.
31. Guan, L., and Kaback, H. R. (2007) Site-directed alkylation of cysteine to test solvent accessibility of membrane proteins. *Nat. Protoc. 2*, 2012–2017.
32. Bouillet, P., Sapin, V., Chazaud, C., Messaddeq, N., Decimo, D., Dolle, P., and Chambon, P. (1997) Developmental expression pattern of Stra6, a retinoic acid-responsive gene encoding a new type of membrane protein. *Mech. Dev. 63*, 173–186.
33. Szeto, W., Jiang, W., Tice, D. A., Rubinfeld, B., Hollingshead, P. G., Fong, S. E., Dugger, D. L., Pham, T., Yansura, D. G., Wong, T. A., Grimaldi, J. C., Corpuz, R. T., Singh, J. S., Frantz, G. D., Devaux, B., Crowley, C. W., Schwall, R. H., Eberhard, D. A., Rastelli, L., Polakis, P., and Pennica, D. (2001) Overexpression of the retinoic acid-responsive gene Stra6 in human cancers and its synergistic induction by Wnt-1 and retinoic acid. *Cancer Res. 61*, 4197–4205.
34. Sun, H., Smallwood, P. M., and Nathans, J. (2000) Biochemical defects in ABCR protein variants associated with human retinopathies. *Nat. Genet. 26*, 242–246.
35. Hediger, M. A., Romero, M. F., Peng, J. B., Rolfs, A., Takanaga, H., and Bruford, E. A. (2004) The ABCs of solute carriers: Physiological, pathological and therapeutic implications of human membrane transport proteinsIntroduction. *Pfluegers Arch. 447*, 465–468.

BI8002082